Comparisons between the TAO Buoy and NASA Scatterometer Wind Vectors

SUZANNE DICKINSON AND KATHRYN A. KELLY

Applied Physics Laboratory, University of Washington, Seattle, Washington

MICHAEL J. CARUSO

Department of Physical Oceanography, Woods Hole Oceanographic Institution, Woods Hole, Massachusetts

MICHAEL J. MCPHADEN

NOAA/Pacific Marine Environmental Laboratory, Seattle, Washington

30 August 1999 and 5 September 2000

ABSTRACT

There was an opportunity to compare 10 months of collocated National Aeronautics and Space Administration scatterometer (NSCAT) wind vectors with those from the Tropical Atmosphere Ocean (TAO) buoy array, located in the tropical Pacific Ocean. Over 5500 data pairs, from nearly 70 buoys, were collocated in the calibration/validation effort for NSCAT. These data showed that the wind speeds produced from the NSCAT-1 model function were low by about 7%–8% compared with TAO buoy winds. The revised model function, NSCAT-2, produces wind speeds with a bias of about 1%. The scatterometer directions were within 20° (rms), meeting accuracy requirements, when compared to TAO data. The mean direction bias between the TAO and the NSCAT vectors (regardless of model function) is about 9° with the scatterometer winds to the right of the TAO winds, which may be due to swell. The statistics of the two datasets are discussed, using component biases in lieu of the speed bias, which is naturally skewed. Using ocean currents and buoy winds measured along the equator, it is shown that the scatterometer measures the wind relative to the moving ocean surface. In addition, a systematic effect of rain on the NSCAT wind retrievals is noted. In all analyses presented here, winds less than 3 m s^{-1} are removed, due to the difficulty in making accurate low wind measurements.

1. Introduction

Wind vector data from the Tropical Atmosphere Ocean (TAO) buoy array were used as part of the calibration/validation effort to evaluate the National Aeronautics and Space Administration (NASA) scatterometer (NSCAT) wind vector data measured from the polar-orbiting Advanced Earth Observing Satellite (ADEOS I). Ten months of NSCAT swath data from September 1996 through June 1997 were collected in two 600-km-wide bands on either side of an approximately 325-km-wide nadir gap. The resolution of the NSCAT data is 25 km, with required accuracies for speed of 2 m s^{-1} (rms) for 3–20 m s^{-1}, 10% for 20–30 m s^{-1} and 20° (rms) for direction (Jet Propulsion Laboratory 1998). The scatterometer measures winds in all weather conditions and covers 90% of the ice-free oceans every two days.

The TAO array, consisting of nearly 70 buoys, shown in Fig. 1, spans the Pacific Ocean from 8°S to 8°N (McPhaden et al. 1998), providing a unique opportunity to calibrate NSCAT winds over the open ocean in the Tropics. TAO wind vectors are measured hourly [with an accuracy of 0.3 m s^{-1} or 3%, whichever is larger, for speed, and a preliminary estimate of 7° for direction accuracy (P. Freitag 2000, personnal communication)] along with air, sea surface and subsurface temperatures, and relative humidity. Several buoys also measure ocean currents on the equator, and others measure rainfall. The subsurface temperature data are not relevant to this study and, due to a lack of collocated rainfall measurements, TAO rainfall data are not used.

To make the most direct comparison, we collocated NSCAT and TAO data within 30 min and 25 km of each other, consistent with the findings of Gilhousen (1987). Since the NSCAT model function produces a wind at 10 m, assuming a neutrally stratified atmosphere, the TAO wind data were converted from 4 m above sea

Corresponding author address: Ms. Suzanne Dickinson, Applied Physics Lab., University of Washington, Box 35-5640, Seattle, WA 98195.
E-mail: suzanne@apl.washington.edu

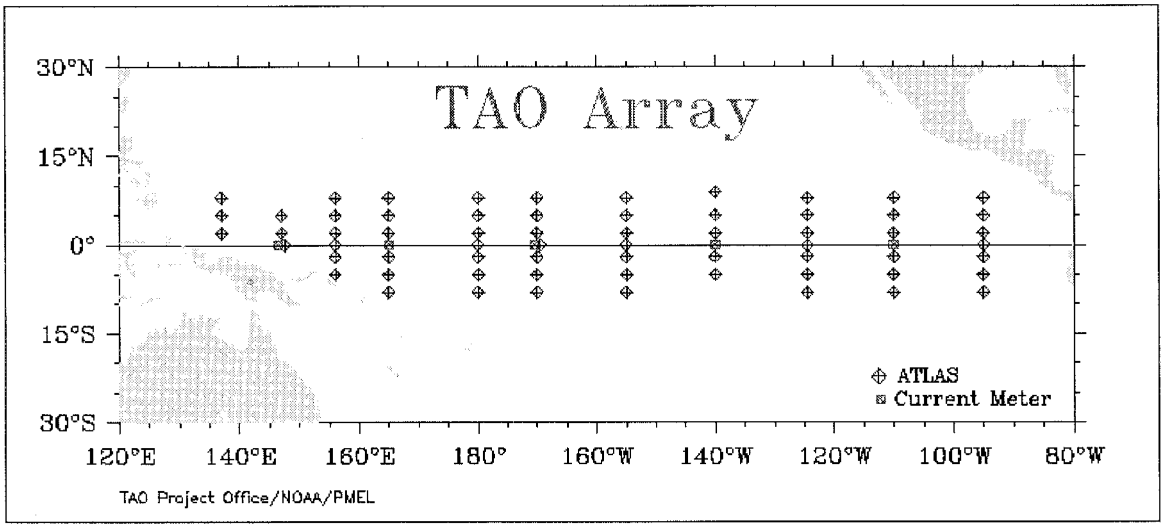

FIG. 1. TAO buoy array spanning the equatorial Pacific Ocean. There are 67 buoys in the array with approximately 5 equipped with current meters.

level in the real atmosphere to 10 m in a neutrally equivalent atmosphere. The conversion was made with the bulk formulation of the log profile approximation in the atmospheric surface layer (Liu et al. 1979) using the air temperature, sea surface temperature, and relative humidity data from the TAO moorings. The direction of the wind is assumed not to change with this conversion. On average, the wind speed at 10 m is about 9% larger than that of a wind at 4 m. Two versions of the NSCAT winds were examined: NSCAT-1 (Wentz and Smith 1999), the first postlaunch algorithm, and NSCAT-2. The NSCAT-2 model function primarily increased the wind speeds after comparisons with TAO and other buoys and with ship observations showed that the NSCAT-1 speeds were low (D. Smith 1999, personal communication). Details of the buoy–scatterometer collocated dataset used for this study are given in Caruso et al. (1999).

2. Wind speed, wind component, and wind direction statistics

The simplest comparison between the two wind datasets would seem to be a comparison of wind speeds. However, there are several issues that complicate this comparison. First, we note that TAO measures and vector averages wind components at a 2-Hz rate, and records one 6-min average per hour, centered at the top of the hour. The scatterometer, on the other hand, is a scalar measuring device. Scalar averaging generally results in higher speeds than vector averaging. Using TAO wind data at the hour prior to and following the scatterometer pass, the winds are both vector averaged and scalar averaged. The vector-averaged wind speeds are less than 1% lower than the scalar-averaged speeds, showing the steadiness of the equatorial winds. The scatterometer also measures a spatial average of the wind speed over a 25-km footprint. With a 6-m s^{-1} average wind speed, a parcel crosses a scatterometer footprint in approximately 70 min. To reduce the impact of the spatial variability of the wind over the footprint, we averaged the TAO data at the hour prior to and following the satellite pass.

A different type of problem in comparing wind speeds is that wind speed cannot be negative. Speed errors therefore cannot vary normally about the speeds, particularly near zero. The result is a more positive bias at low wind speeds, skewing the overall mean bias (Freilich 1997). The speed comparison between NSCAT-1 and TAO (Fig. 2a, circles) suggests that NSCAT-1 wind speeds are generally low relative to the TAO winds, although for the lowest wind speeds the bias appears to be positive. A simple simulation of the speed bias is presented below to illuminate this issue. However, we first examine the components that give a more straightforward comparison, as they can be both positive and negative, and have errors that can vary normally about the mean value.

Zonal and meridional components of collocated wind vectors from NSCAT and TAO were compared when speeds were greater than 3 m s^{-1}, as the scatterometer wind direction error increases with decreasing wind speeds (Freilich and Dunbar 1999). For each vector we selected only the larger of the two components because the smaller component contains a relatively larger fraction of the direction error. The component scatterplots between TAO and NSCAT-1 (Fig. 3 left-hand panels) show that both zonal and meridional NSCAT-1 components are smaller than their TAO counterparts. The component bias is a function of the magnitude of the component itself; that is, the NSCAT-1 zonal wind u_s can be estimated as a linear function of the TAO zonal

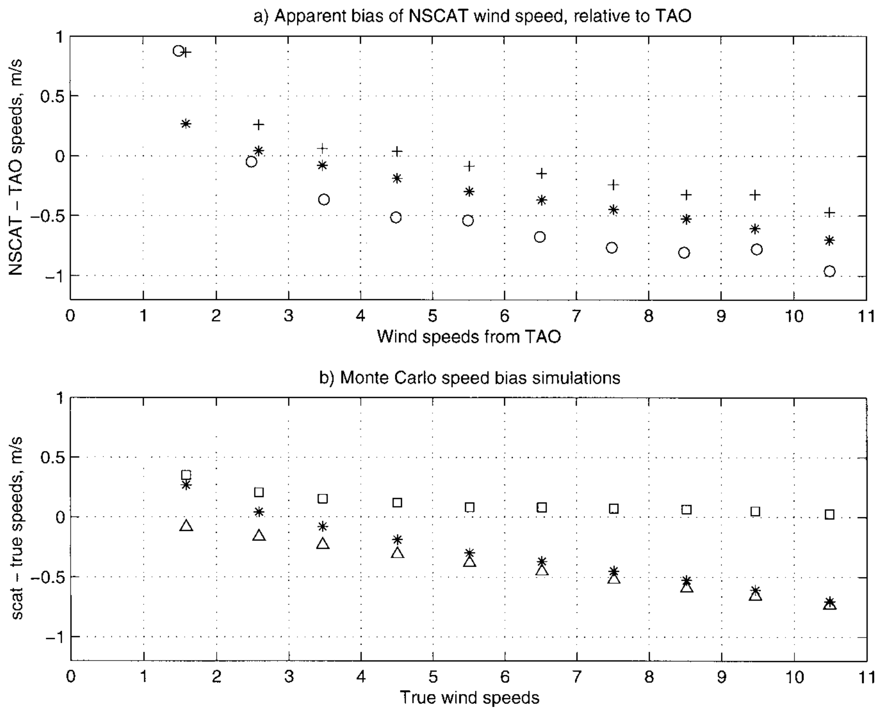

FIG. 2. Wind speed bias between NSCAT and TAO winds. (a) NSCAT speed minus TAO buoy speed for NSCAT-1 (open circles), NSCAT-2 (pluses), and a simulation of NSCAT-1 speed errors (asterisks). (b) Biases from Monte Carlo simulation of NSCAT-1 errors: real bias (triangles), artificial bias (squares), and apparent bias (asterisks). See text for discussion of artificial bias estimate.

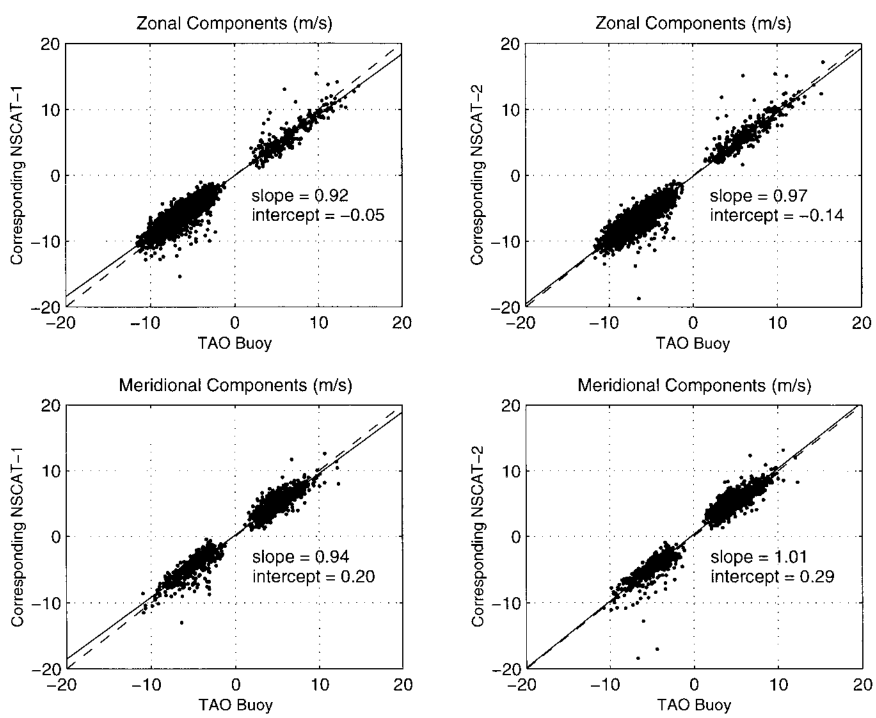

FIG. 3. Wind component scatterplots, (left) TAO vs NSCAT-1 and (right) TAO vs NSCAT-2. Data were plotted only if NSCAT and TAO vectors were within 30° of each other and wind speeds were greater than 3 m s^{-1}. Then only the larger of the two components was used. The solid line shows best linear fit with slope and intercept listed in each plot. The dashed line shows a perfect fit.

wind u_b, as $u_s = \alpha u_b$, where $\alpha = 0.92$, plus a negligible offset. The meridional winds have a similar relationship with $\alpha = 0.94$. The NSCAT-2 components have a slope (α) of approximately 1 relative to the TAO components in the scatterplots (right-hand panels of Fig. 3).

The simple NSCAT-1 component bias, in conjunction with random errors in the components, produces a complicated speed bias. The complication arises because the speed is derived from the square of the components, which also squares the component errors. While the mean of the component errors may be zero, the mean of the squared errors is always positive.

To explain the structure of the speed bias, we take a simple example in which there is no bias in the components, that is, $\alpha = 1$. We assume that the buoy wind vector $\mathbf{u}_b = (u, v)$ has no error and that the scatterometer wind vector $\mathbf{u}_s$ has errors ϵ which have zero mean, $\mathbf{u}_s = (u + \epsilon_u, v + \epsilon_v)$. The NSCAT speed then becomes

$$s_s^2 = u^2 + 2u\epsilon_u + \epsilon_u^2 + v^2 + 2v\epsilon_v + \epsilon_v^2,$$

where $s^2 = u^2 + v^2$ and s is the buoy wind speed. We further assume, consistent with the lack of a component bias, that the errors are not correlated with the true wind components, that is, $\langle u\epsilon_u \rangle = \langle v\epsilon_v \rangle = 0$, where $\langle\ \rangle$ is an ensemble average. Then the difference of the squared speeds is given by

$$\langle s_s^2 - s^2 \rangle = \langle \epsilon_u^2 \rangle + \langle \epsilon_v^2 \rangle,$$

which is simply the sum of the squared component errors. Assuming the component errors have the same average magnitude ϵ_0, then

$$\langle s_s^2 - s^2 \rangle = 2\epsilon_0^2,$$

where $\langle s_s - s \rangle$ is the artificial speed bias, which is always positive because s_s is greater than s. This bias is an artifact of using speed for the comparisons and is instead a measure of the root-mean-square difference between wind components, rather than a true bias. Note that if the NSCAT winds were assumed to have no error and there was no real bias ($\alpha = 1$), then the TAO buoy speeds would appear to be larger than NSCAT speeds.

To illustrate the error structure as a function of true wind speed, a Monte Carlo simulation of the errors was conducted, first using winds with no real bias ($\alpha = 1$), but adding random errors to estimate the artificial bias. Next, the same analysis was done using the real bias of NSCAT-1 components ($\alpha = 0.93$). The real speed bias determined from the component comparison is shown in Fig. 2b (triangles). The artificial bias, which arises from random errors (here, $\epsilon_0 = 1.0$) is also shown in Fig. 2b (squares). Finally, the apparent bias, which is real bias plus artificial bias, is shown in both Figs. 2a and 2b (asterisks). A comparison of the simulated (apparent) bias (asterisks) and the computed bias (circles) in Fig. 2a suggests that the positive bias at low wind speeds comes from the random errors in the components. The simulated bias (asterisks) is smaller than observed at the lowest wind speeds; this finding is consistent with the relatively larger direction discrepancies observed at low wind speeds (Caruso et al. 1999). The plus symbols in Fig. 2a represent the computed bias for NSCAT-2 wind speeds.

The direction bias for both the NSCAT-1 and NSCAT-2 model functions is approximately 9° with the NSCAT vectors to the right of the TAO wind vectors and is currently unexplained. We checked all other variables in our collocated dataset for a dependence on directional bias. We looked for direction dependence on the Coriolis turning in the Ekman layer of the atmosphere (direction bias as a function of latitude). We also looked for directional bias being related to scanning geometry characteristics, or as a function of the geophysical variables available from the TAO buoys, including atmospheric stratification. We found no strong relationships with direction bias.

Perhaps the direction bias is due to ocean swell. Reider et al. (1994) found the stress direction (scatterometers actually measure stress and not wind) to be influenced by long waves, where the direction of the stress falls between the wind direction and the direction of the long waves. Essen (1999) found evidence that the direction error in the model function of the *ERS-1* scatterometer can be more than 20° in the presence of swell. Rufenach et al. (1998) suggested that swell in the equatorial Pacific Ocean is the cause of a 10° difference in the directions between the *ERS-1* scatterometer and the TAO buoys, again with scatterometer winds to the right of buoy winds. This direction bias is similar to that found when the NSCAT data were compared to National Data Bouy Center buoy winds (Freilich and Dunbar 1999) and Special Sensor Microwave Imager (SSM/I) winds (Wentz and Smith 1999). Unfortunately, no wave data are taken on TAO buoys. Swell in the equatorial Pacific may be the main cause of the direction discrepancies between the scatterometer and the TAO buoys and deserves more study.

The mission requirements for the NASA scatterometer are listed in Table 1. The accuracy requirement for wind speed is 2 m s^{-1} (rms) for 3–20 m s^{-1} and 10% for winds 20–30 m s^{-1}. The accuracy requirement for wind direction is for the *closest* vector to be within 20°(rms) for a speed range of 3–30 m s^{-1} (Naderi et al. 1991). The NASA scatterometer met the mission requirements when compared to TAO buoy data within 25 km and 30 min of the scatterometer measurement. There were no scatterometer or TAO buoy wind speeds above 20 m s^{-1} in this study. Other comparison statistics for the 3–20 m s^{-1} range are also included in Table 1. As discussed above, the speed bias and component slopes improved with the NSCAT-2 model function. The direction bias remained basically the same. The rms difference for speed also improved with NSCAT-2. The direction rms for the selected vectors (those chosen with the ambiguity removal algorithm) are relatively large compared to the closest vector (closest to truth).

TABLE 1. Comparison statistics, 3–20 m s^{-1}.

Model function	Sample size	Speed (m s^{-1}) Mission requirement rms	Speed Selected vector Rms	Speed Selected vector Bias	Components (m s^{-1}) Zonal slope	Components Meridional slope	Direction (°) Mission requirement rms	Direction Closest vector* rms	Direction Selected vector** Rms	Direction Selected vector** Bias
NSCAT-1	5106	2.0	1.28	−0.56	0.92	0.94	20	19.0	35.0	9.1
NSCAT-2	5718	2.0	1.14	−0.07	0.97	1.01	20	19.5	32.7	9.2

* The ambiguity closest in direction to the ''truth.''
** The vector chosen by the ambiguity removal algorith.

3. Effect of ocean currents on NSCAT wind estimates

Three TAO buoys located along the equator at 165°E, 140°W, and 110°W measured ocean currents during the NSCAT period. This gave us the opportunity to examine the effect of the ocean currents on scatterometer measurements relative to the buoy measurements. We know that the scatterometer backscatter is due to the wind stress acting on and roughening the ocean surface. The scatterometer, therefore, is measuring winds relative to the moving ocean surface, rather than winds relative to a fixed location, as an anemometer does. Thus, NSCAT winds should be weaker than TAO winds when currents are in the same direction as the wind and should be stronger when ocean currents oppose the wind. Halpern (1988) noted this effect on computed surface stress, where the surface stress decreased (increased) for winds in the same (opposite) direction as currents. To test the influence of ocean currents on the scatterometer measurements, the hourly ocean current vectors with accuracies of approximately 4–7 cm s^{-1} (Halpern 1987) were obtained from the current meters on the TAO moorings mentioned above. There were 238 collocated pairs of NSCAT-2 and TAO wind data for which currents at a depth of 10 m were available and the winds were greater than 3 m s^{-1}. To eliminate conditions of rapidly changing winds or currents, collocated data for which ocean currents changed direction by more than 40° or magnitude by more than 0.10 m s^{-1} in one hour were removed. Similarly, collocated data for which TAO 10-m winds changed direction by more than 40° or magnitude by more than 3.0 m s^{-1} in one hour were also removed. This screening eliminated 12 pairs of data. In addition, collocated pairs for which TAO and NSCAT-2 directions differed by more than 60° were eliminated (10 pairs). This gave 216 collocated wind and current vector triplets (Fig. 4).

This analysis is complicated by the wind vector direction bias (perhaps induced by swell), as described in the previous section. However, the winds and currents are primarily zonal as shown in Figs. 4a and 4b, suggesting that a comparison of the zonal wind differences with zonal currents would be the most straightforward. To minimize the effect of the direction discrepancies on this analysis, proxy NSCAT zonal winds were obtained by combining the NSCAT-2 wind speeds with TAO wind directions for all 216 collocated data pairs.

Zonal wind differences were computed by subtracting the NSCAT-2 proxy zonal wind components from the TAO zonal winds. A correlation was then computed between the differences in the zonal wind components and the zonal component of the current, when the wind speeds were greater than 3 m s^{-1}; the scalar correlation was 0.58 (95% significance level was 0.40). An alternative explanation of a correlation between wind differences and currents is that the winds are driving the currents, and the wind difference simply reflects an underestimation of the winds by NSCAT-2 ($\langle u_s^2 \rangle = \alpha \langle u_b^2 \rangle$, where $\alpha < 1$); if this were the case, the difference would actually be between $(1 - \alpha)$ times the buoy wind speed and ocean currents. To test this null hypothesis, a scalar correlation between zonal currents and zonal TAO winds was computed. The resulting correlation was 0.43, nearly as high as for the differences, but the 95% significance level in this case was 0.57, so that the correlation was not significant. (The higher significance level reflects the relatively low variability of the TAO winds, compared with the wind differences.) Therefore, currents account for roughly one-third of the variance in the zonal wind differences.

This comparison suggests that the scatterometer that measures stress is estimating a wind speed relative to the ocean surface; therefore, caution is needed in using winds over strong ocean currents for the calibration and validation of scatterometer winds. In most major current systems, winds and currents are roughly aligned, so that the scatterometer would be measuring a lower wind speed than an anemometer. The regression coefficient of the difference in the 10-m winds on the currents is 1.3. So, for a 1 m s^{-1} current speed, typical of a western boundary current, and a 10-m wind speed of 10 m s^{-1}, the scatterometer 10-m wind would be about 8.7 m s^{-1}, compared with an anemometer wind of 10 m s^{-1}, a reduction of more than 10%. During the NSCAT mission, the equatorial currents reversed during the onset of the 1997 El Niño, so that currents opposed the winds for half of the data record and were aligned with the winds for the other half. Therefore, on average, the energetic equatorial currents contributed little to a speed bias in NSCAT.

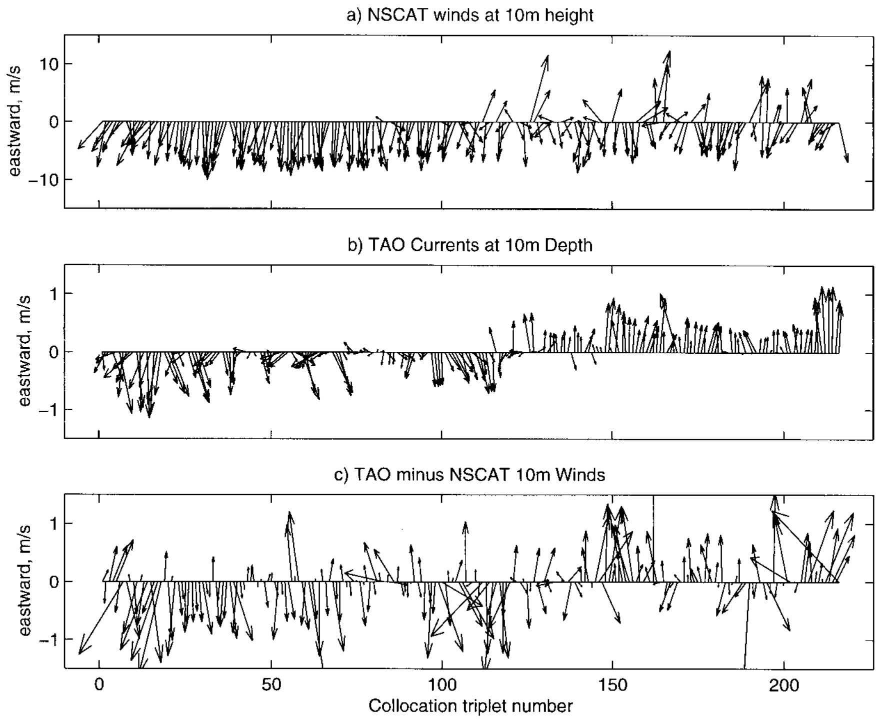

FIG. 4. Effect of ocean currents on NSCAT winds. (a) NSCAT-2 winds (eastward is up). (b) Currents at a depth of 10 m measured from TAO buoys. (c) The difference between TAO buoy and NSCAT-2 vectors at the ocean surface. The difference between the TAO and NSCAT-2 wind speeds is significantly correlated with the component of the ocean currents in the direction of the buoy winds.

4. Rain effect on NSCAT wind stress estimates

The wind data from the TAO array are presumably not effected by rain. The NSCAT sensor, however, measures the ocean surface roughness. There are two possible effects of rain: attenuation of the backscatter signal by the rainwater in the atmosphere, resulting in wind speeds that are too low; or increased ocean surface roughness that reflects more of the signal back to the satellite, resulting in wind speeds that are too high. Smith and Wentz (1998) have shown that the former process dominates in regions of high winds and the latter process dominates in regions of low winds, such as the Tropics. In this region, the increase in roughness should dominate the effects of signal attenuation by the rain. Here we compare the difference between monthly averaged TAO wind stresses and monthly averaged NSCAT stresses at the buoy locations (for wind speeds greater than 3 m s^{-1}) with monthly precipitation estimates. Monthly means are used because sufficient collocations of rain estimates, NSCAT, and TAO winds are not available.

The monthly precipitation fields used for this analysis were obtained from the National Oceanic and Atmospheric Administration (NOAA) National Centers for Environmental Prediction (Xie and Arkin 1997). They are a merged dataset composed of rain gauge data as well as several satellite-derived precipitation datasets, including the outgoing longwave radiation–based precipitation index, the Microwave Sounding Unit, the Geostationary Operational Environmental Satellite Precipitation Index, and two SSM/I products. We use the version of monthly precipitation rate that did not include numerical model output. The spatial grid for this global monthly product is 2.5° × 2.5°. The precipitation product was interpolated to a 1° × 1° grid, to obtain the values at the TAO buoy locations.

A gridded stress product from the NSCAT-2 data (Kelly et al. 1999) covering the tropical Pacific Ocean from 30°S to 30°N is used in the following comparisons with TAO data. Stress is considered, as it is the variable that forces ocean models and quantifies momentum transfer across the air–sea interface. The maps have 5-day and 2° resolutions and are available daily from 1 November 1996 through 26 June 1997 on a 1° grid. Pseudostress maps (stress with drag coefficient and density values of one) were converted to stress ($C_d = 1.2 \times 10^{-3}$) and averaged over each month from November 1996 to June 1997. The hourly winds from the TAO buoys were also converted to stress using the same drag coefficient and averaged over each month. We compare the mapped precipitation and NSCAT stress at the grid point closest to each TAO buoy.

NSCAT-2 stress magnitudes were generally larger than TAO values along 5° and 8°N, and between 155°

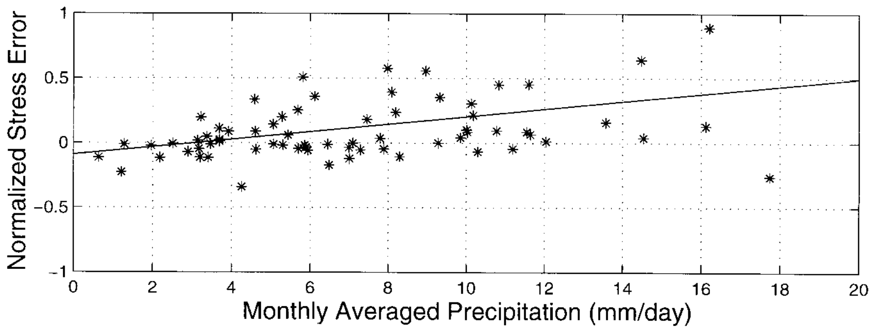

FIG. 5. Normalized stress magnitude error ([(NSCAT-2) − TAO]/TAO) as a function of precipitation rate. The scatterplot includes monthly averaged data from buoys at 5° and 8°N (the ITCZ region). The solid line is the best fit to the data and suggests that a precipitation rate of 10 mm day^{-1} will cause about a 20% overestimation in stress.

and 95°W, the heavy precipitation region of the intertropical convergence zone (ITCZ), for November 1996–February 1997 and for May–June 1997. NSCAT-2 stress magnitudes were both larger and smaller in other areas of the tropical Pacific Ocean and for other months, varying by as much as a factor of 2. Figure 5 shows the normalized error of the magnitude of the stress {[(NSCAT-2) − TAO]/TAO} for the NSCAT period for 5° and 8°N versus the monthly precipitation rate. The error increases with the rain rate, with an approximately 20% overestimation of stress at an average rain rate of 10 mm day^{-1}. The ITCZ is a region where the curl of the wind stress plays an important role in ocean dynamics (Sverdrup 1947) and where NSCAT winds differ markedly from wind products such as from the European Centre for Medium-Range Weather Forecasts analyses (Kelly et al. 1999). These differences have a significant impact on numerical model simulations of the Pacific North Equatorial Countercurrent (Yu and Moore 2000); thus, it is critical that a provision is made for detecting or correcting for precipitation in scatterometer measurements.

5. Summary and conclusions

We presented the results of a calibration exercise for the NASA scatterometer. We analyzed NSCAT wind vector data with respect to data from the TAO buoy array in the equatorial Pacific Ocean for wind speeds greater than 3 m s^{-1}. NSCAT-1 winds were found to be 7%–8% low, while the improved NSCAT-2 wind speeds have effectively no bias. The NSCAT vectors from both model functions were on average about 9° to the right of the TAO vectors, consistent with the thought that swell influences scatterometer directions. The NSCAT wind vectors met mission requirements by being within 2 m s^{-1} (rms) in speed and 20° (rms) in direction when compared to TAO buoy winds within 25 km and 30 min of a scatterometer measurement.

Wind speed bias was shown to have an inherent artificial component, skewing the mean bias to a more positive value, due to the non-negativity of speed itself. Also, the differences between the TAO and NSCAT winds showed that the scatterometer measures the stress relative to the moving ocean surface. NSCAT speeds are lower (higher) than buoy winds over fast currents in the same (opposite) direction as the wind. Rain on the ocean surface was found to affect the estimated wind speeds in the ITCZ region of high rainfall. The wind stresses were high by about 20% in areas of high rain rate.

Acknowledgments. The authors would like to thank F. Wentz and D. Smith for helpful comments regarding the scatterometer bias and the effects of precipitation, and Z.-J. Yu for recognizing this effect in our wind fields. The TAO buoy program and data are maintained by the Pacific Marine Environmental Laboratory (PMEL) at the National Oceanic and Atmospheric Administration, in collaboration with institutions in Japan, France, and Taiwan. In particular, we appreciate the efforts of Paul Freitag from PMEL for providing quality data. Funding for this work was provided by the National Aeronautics and Space Administration, through the NASA Scatterometer (NSCAT) Science Working Team, Contracts 960927 and 960731 with the University of Washington, and by NOAA's Office of Oceanic and Atmospheric Research.

REFERENCES

Caruso, M. J., S. Dickinson, K. A. Kelly, M. Spillane, L. Mangum, M. J. McPhaden, and L. Stratton, 1999: Evaluation of NSCAT scatterometer winds using equatorial Pacific buoy observations. Woods Hole Oceanographic Institution Tech. Rep. 99-10, 64 pp.

Essen, H. H., 1999: Biases in wind-retrieval by empirical ERS-1/2 scatterometer models due to the presence of long ocean waves. *Proc. Int. Geoscience and Remote Sensing Symp.,* Hamburg, Germany, IEEE, **3,** 1637–1639.

Freilich, M. H., 1997: Validation of vector magnitude datasets: Effects of random component errors. *J. Atmos. Oceanic Technol.,* **14,** 695–703.

——, and R. S. Dunbar, 1999: The accuracy of the NSCAT 1 vector winds: Comparisons with National Data Buoy Center buoys. *J. Geophys. Res.,* **104,** 11 231–11 246.

Gilhousen, D. B., 1987: A field evaluation of NDBC moored buoy winds. *J. Atmos. Oceanic Technol.,* **4,** 94–104.

Halpern, D., 1987: Comparison of upper ocean VACM and VMCM observations in the equatorial Pacific. *J. Atmos. Oceanic Technol.,* **4,** 84–93.

——, 1988: Moored surface wind observations at four sites along the Pacific equator between 140°W and 95°W. *J. Climate,* **1,** 1251–1260.

Jet Propulsion Laboratory, 1998: NASA scatterometer science data product (NSCAT–2) user's manual: Overview and geophysical data products. JPL Publication D-12985, Pasadena, CA, 78 pp.

Kelly, K. A., S. Dickinson, and Z.-J. Yu, 1999: NSCAT tropical wind stress maps: Implications for improving ocean modeling. *J. Geophys. Res.,* **104,** 11 291–11 310.

Liu, W. T., K. B. Katsaros, and J. A. Businger, 1979: Bulk parameterization of air–sea exchanges of heat and water vapor including the molecular constraints at the interface. *J. Atmos. Sci.,* **36,** 1722–1735.

McPhaden, M. J., and Coauthors, 1998: The Tropical Ocean–Global Atmosphere (TOGA) observing system: A decade of progress. *J. Geophys. Res.,* **103,** 14 169–14 240.

Naderi, F. M., J. H. Freilich, and D. G. Long, 1991: Spaceborne radar measurement of wind velocity over the ocean—An overview of the NSCAT scatterometer system. *Proc. IEEE,* **79,** 850–866.

Rieder, K. F., J. A. Smith, and R. A. Weller, 1994: Observed directional characteristics of the wind, wind stress, and surface waves on the open ocean. *J. Geophys. Res.,* **99,** 22 589–22 596.

Rufenach, C. L., J. J. Bates, and S. Tosini, 1998: ERS-1 scatterometer measurements—Part 1: The relationship between radar cross section and buoy wind in two oceanic regions. *IEEE Trans. Geosci. Remote Sens.,* **36,** 603–622.

Smith, D. K., and F. J. Wentz, 1998: Correction of rain affected NSCAT winds. *Eos, Trans. Amer. Geophys. Union,* **79,** (Fall Meeting Suppl.), F17.

Sverdrup, H. U., 1947: Wind-driven currents in a baroclinic ocean, with application to the equatorial currents of the eastern Pacific. *Proc. Natl. Acad. Sci. U.S.A.,* **33,** 318–326.

Wentz, F. J., and D. K. Smith, 1999: A model function for the ocean-normalized radar cross section at 14 GHz derived from NSCAT observations. *J. Geophys. Res.,* **104,** 11 499–11 514.

Xie, P., and P. A. Arkin, 1997: Global precipitation: A 17-year monthly analysis based on gauge observations, satellite estimates, and numerical model output. *Bull. Amer. Meteor. Soc.,* **78,** 2539–2558.

Yu, Z.-J., and D. W. Moore, 2000: Validating the NSCAT winds in the vicinity of the Pacific Intertropical Convergence Zone. *Geophys. Res. Lett.,* **27,** 2121–2124.